

# Moisture Induced Damage in Oxide Scales

M. Rudolphi, M. Schütze  
e-mail: rudolphi@dechema.de  
Funded by: DFG  
Period: 01.04.2009 - 31.09.2011

Deutsche  
Forschungsgemeinschaft  
**DFG**

## Introduction

Water vapor is present in most environments used in high temperature applications. The water vapor content can vary from a few vol.% for example in coal combustion environments, to as much as 100 vol.% in steam turbines. The effect of water vapor on oxide scale growth has been the focus of high temperature materials research for over a decade, revealing for example increased growth rates or more pronounced inward growing oxides in the presence of water vapor. However, the effects of water vapor and liquid water on oxide scale integrity and mechanical properties have, up to now, not been investigated in detail, even though a few reports exist that show increased alumina scale spallation on contact with liquid water [1, 2]. Also, moisture induced failure of thermal barrier coatings has been reported [3, 4]. Since high-technology materials used in high temperature applications rely on protective oxide scales, a loss of the protective oxide limits the materials life time and has to be avoided.

The aim of this study is therefore to investigate the effect of water vapor on the mechanical integrity of typical metal oxides found in high temperature environments.

## Theoretical Approach

The mechanical stability of oxide scales is strongly influenced by the physical defect structure present in the scale. Consequently, the critical strain  $\epsilon_c$  to cause oxide scale failure (i.e. delamination or spallation) in a mechanical loading condition will decrease with increasing defect size  $c$ . The characteristics of the critical strain can be modeled for each failure mode using the advanced Oxide Scale Failure Model [5] based on the classical theory from Griffith [6]:

$$\begin{aligned} \text{interfacial cracking / beginning of delamination} & \quad \epsilon_c^{\text{tension}} = \frac{\eta^{\text{t}}}{(1+\frac{\nu}{2})\sqrt{\frac{c_0}{c}}}, \quad \eta^{\text{t}} = \frac{K_{Ic}(1+\nu)}{2fE\sqrt{\pi c_0}}, \quad \epsilon_c^{\text{compression}} = \frac{\eta^{\text{c}}}{(1+\frac{\nu}{2})\sqrt{\frac{c_0}{c}}}, \quad \eta^{\text{c}} = -\frac{K_{Ic}(1+\nu)}{2fE\sqrt{\pi c_0}} \\ \text{through cracking} & \quad \epsilon_c^{\text{t}} = \frac{\eta^{\text{t}}}{\sqrt{\frac{c_0}{c}}}, \quad \eta^{\text{t}} = \frac{K_{Ic}}{fE\sqrt{\pi c_0}}, \quad \epsilon_c^{\text{sh}} = \frac{\eta^{\text{sh}}}{\sqrt{\frac{c_0}{c}}}, \quad \eta^{\text{sh}} = -\frac{K_{Ic}\sqrt{3}}{fE\sqrt{\pi c_0}} \end{aligned}$$

$c$  – defect size,  $c_0$  – 1  $\mu\text{m}$  for normalizing,  $E$  – scale Young's modulus,  $f$  – defect geometry factor,  $r$  – interface roughness,  $\nu$  – poisson ratio,  $K_{Ic}$  – scale fracture toughness

## Experimental

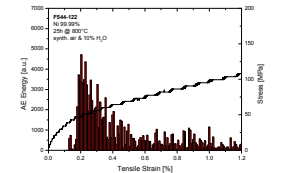
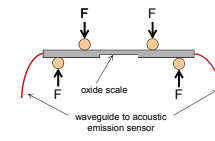
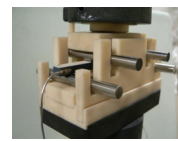


Figure 1: Photograph and schematics of the 4-pt. bend specimen fixture (top) and typical measurement results (bottom).

## Mechanical 4-Point Bending

High purity Nickel (99.99%) and Titanium (99.6%) were used as substrate materials in an attempt to form oxide scales with a minimum amount of impurities. High temperature oxidation was performed at 800°C in dry synthetic air and humid synthetic air with 10 Vol.% H<sub>2</sub>O for durations of up to 100 hours. 4-point bending with in-situ acoustic emission measurement was carried out at room temperature to examine the mechanical properties of the oxide scales formed by high temperature oxidation.

## Nickel Oxide

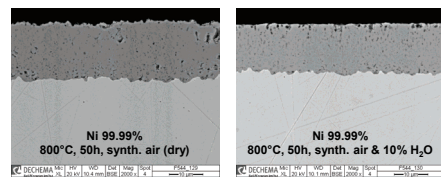


Figure 2: SEM micrographs of high purity Ni after 50h oxidation at 800°C in dry (left) and humid (right) atmosphere, respectively.

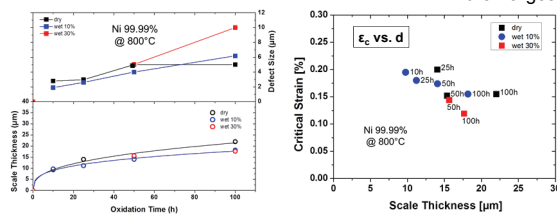
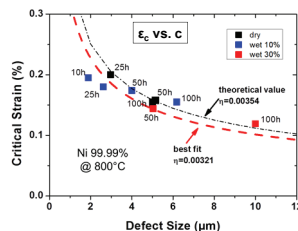


Figure 4: Physical defect kinetics (top left) and oxide scale growth kinetics (bottom left) and "classical" scale failure diagram (right) for nickel oxide.



advanced oxide scale failure diagrams  $\epsilon_c$  vs.  $c$  using the new approach are compared. No clear trend is observed for Ni in the classical approach, however, there is a clear tendency to be seen in the advanced oxide scale failure diagram (OSFD) given in figure 6. Furthermore, the measured data is in reasonable agreement with the theoretical value and no significant effect of water vapor can be observed for nickel oxide. In the case of Ti a distinct difference between humid and dry oxidized specimens can be observed in the advanced OSFD (see figure 7), whereas in the classical diagram (figure 5b) this information is not evident.

Figure 6: Advanced oxide scale failure diagram for nickel oxide.

## Summary

### Nickel oxide

- Scale growth kinetics is parabolic (only little difference in  $k_p$ , humid / dry)
- Physical defect growth kinetics linear at 800°C, similar for dry / humid
- Clear tendencies in  $\epsilon_c$  vs.  $c$  in contrast to  $\epsilon_c$  vs.  $d$
- No significant effect of water vapor on critical strain

## References

1. J.L. Smialek, G.N. Morscher, Materials Science and Engineering A, 332 (2002) 11.  
2. J.L. Smialek, JOM, 58 (2006) 29.  
3. J.L. Smialek, D. Zhu, and M.D. Cuy, Scripta Materialia, 59 (2008) 67.

## Results

The SEM micrographs of the nickel samples shown in figure 2 reveal a slightly thicker oxide scale for humid oxidation and only minor differences in defect structure between dry and humid oxidation. In contrast, titanium forms oxide scales of quite different microstructure when oxidized in dry and humid environment, respectively, as can be seen in figure 3. While oxidation in dry synthetic air leads to a layered microstructure, oxidation in 10 vol.% H<sub>2</sub>O results in a compact scale with much fewer defects. Since the largest defects will be most likely to cause scale failure (i.e. spallation or delamination) the size  $c$  of the largest defects visible in the SEM micrographs was

extracted from the SEM images as a function of oxidation time (see figures 4a and 5a). Also, the oxide scale thickness was measured from the micrographs. This data, in combination with the critical strain values from the 4-point bending enables to plot the "classical" form of an oxide scale failure diagram (figures 4b and 5b). However, the classical  $\epsilon_c$  vs.  $d$  - diagrams fail to describe these systems properly. This becomes obvious when the

advanced oxide scale failure diagrams  $\epsilon_c$  vs.  $c$  using the new approach are compared. No clear trend is observed for Ni in the classical approach, however, there is a clear tendency to be seen in the advanced oxide scale failure diagram (OSFD) given in figure 6. Furthermore, the measured data is in reasonable agreement with the theoretical value and no significant effect of water vapor can be observed for nickel oxide. In the case of Ti a distinct difference between humid and dry oxidized specimens can be observed in the advanced OSFD (see figure 7), whereas in the classical diagram (figure 5b) this information is not evident.

Figure 7: Advanced oxide scale failure diagram for titanium oxide.

## Titanium Oxide

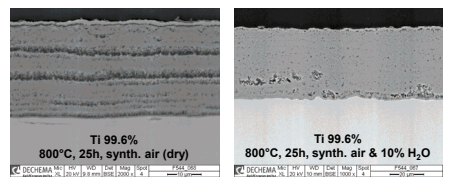


Figure 3: SEM micrographs of high purity Ti after 50h oxidation at 800°C in dry (left) and humid (right) atmosphere, respectively.

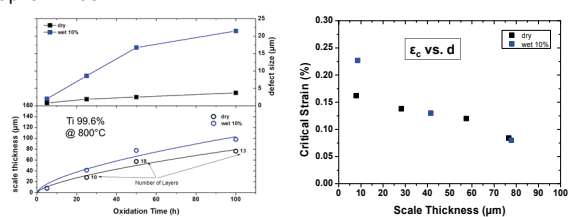
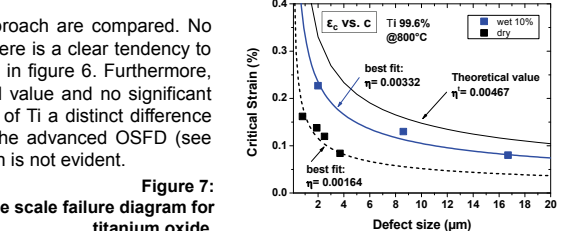


Figure 5: Physical defect kinetics (top left) and oxide scale growth kinetics (bottom left) and "classical" scale failure diagram (right) for titanium oxide.



### Titanium oxide

- Scale growth kinetics is parabolic ( $k_p$  slightly higher in humid)
- Physical defect growth kinetics decelerating with time, faster for humid
- Clear difference between humid / dry in  $\epsilon_c$  vs.  $c$  in contrast to  $\epsilon_c$  vs.  $d$
- Water vapor increases  $\eta$  and  $c$

4. M. Rudolphi, D. Renusch, and M. Schütze, Scripta Materialia, 59 (2008) 255.  
5. Griffith, A.A., Philos. Trans. R. Soc. London, Series A, Vol. 221 (1921) 163-198.  
6. M. Schütze, P.F. Tortorelli, I.G. Wright, Oxid. Met. 73 (2009) 389-418.